Since January 2020 Elsevier has created a COVID-19 resource centre with free information in English and Mandarin on the novel coronavirus COVID-19. The COVID-19 resource centre is hosted on Elsevier Connect, the company's public news and information website.

HOSTED BY

ELSEVIER

CrossMark

Available online at www.sciencedirect.com

ScienceDirect

Radiology of Infectious Diseases 1 (2015) 64–69

www.elsevier.com/locate/jrid

Research article

Imaging manifestations and pathological analysis of severe pneumonia caused by human infected avian influenza (H7N9)☆

Zheng Zeng, Xiang-rong Huang, Pu-xuan Lu*, Xiao-hua Le, Jing-jing Li, De-ming Chen, Jing Yuan, Guo-bao Li, Ying-xia Liu, Bo-ping Zhou

Third People's Hospital of Shenzhen, 518112 Guangdong, China

Received 27 November 2014; accepted 7 January 2015
Available online 2 March 2015

Abstract

Objective: To investigate the imaging and pathological findings of severe pneumonia caused by human infected avian influenza (H7N9), and therefore to further understand and improve diagnostic accuracy of severe pneumonia caused by human infected avian influenza (H7N9).
Methods: The relevant clinical and imaging data of 19 cases, including 10 males and 9 females, with pneumonia caused by human infected avian influenza (H7N9) was retrospectively analyzed. One of the cases had received percutaneous lung biopsy, with the clinical, imaging and pathological changes possible to be analyzed.
Results: The lesions were mainly located at lower lobes and dorsal of lungs, involving multiple lobes and segments. Ground-glass opacities and/or pulmonary opacities were the more often imaging manifestations of severe pneumonia caused by human infected avian influenza (H7N9) in early and evolving phases (19/19,100%). By biopsy following percutaneous lung puncture, exudation of slurry, cellulose, RBC and neutrophils, formation of hyaline membrane, squamous metaplasia and organizing exudates were observable at the alveolar space. Some of alveoli collapsed, and some responded to show compensatory emphysema.
Conclusion: The imaging features of severe pneumonia caused by human infected avian influenza (H7N9) include obvious ground-glass opacity and pulmonary consolidation, mainly at lower lobes and dorsal of lungs, with rapid changes. The cross-analysis of imaging and pathology preliminary can elucidate the pathological mechanisms of ground-glass opacities and pulmonary consolidation of severe pneumonia. Such an intensive study is beneficial to prompt clinicians to observe and evaluate the progress of the disease. In addition, it is also in favor of managing the symptoms and reducing the mortality rate.

Keywords: Pneumonia; Severe cases; Viral; Avian influenza A (H7N9); Radiography; Lungs; Tomography; X-ray computed; Pathogenic manifestations

Human infected avian influenza (H7N9) is an acute respiratory infection caused by H7N9 subtype of avian influenza A virus [1]. The disease was firstly reported in the spring of 2013 in Yangtze River Delta, China [2]. A total of 23 cases of human infected avian influenza (H7N9) was admitted to our hospital from December, 2013 to April, 2014, with 19 cases suffering from severe pneumonia. In this study, we retrospectively analyzed imaging and pathological manifestations of the disease to shed light on its clinical diagnosis, therapeutic efficacy evaluation and prognosis.

1. Materials and methods

1.1. Basic data

The clinical, radiological and pathological data of 19 cases with severe pneumonia caused by human infected avian influenza (H7N9) from December 18, 2013 to April 18, 2014

☆ Foundation project: major project of the knowledge innovation program in Shenzhen. (Serial number: JCYJ20130401164750006). The Medical Research Foundation of Guangdong Province. (Serial number: A2011543).
* Corresponding author.
E-mail address: lupuxuan@126.com (P.-x. Lu).
Peer review under responsibility of Beijing You'an Hospital affiliated to Capital Medical University.

http://dx.doi.org/10.1016/j.jrid.2015.02.003

in Shenzhen Third People's Hospital, China, were collected. All the patients were tested positive to nucleic acid of H7N9 subtype of avian influenza virus by CDC of Guangdong province and Shenzhen city, China, in line with the diagnostic criteria of severe human infected avian influenza. The 19 cases included 10 males and 9 females, aged 31–82 years with a median of 55 years. Two patients had preexisting hypertension; 3 had hypertension and diabetes; 1 had tuberculosis; and 1 had right pulmonary embolism.

1.2. Clinical manifestations

Fever was the most common symptom, found in all 19 cases (100%), and ardent fever (39 °C or above) showed up in 15 patients (78.9%). Cough was also the most common symptom, occurring in all 19 cases (100%), with expectoration in13 cases (68.4%) and 1 case coughing up dark red bloody sputum. Anhelation occurred in 11 cases (57.9%). All patients were admitted to our hospital at d 4–14 after onset, averagely 8.4 days, and received antiretroviral and respiratory supporting therapies.

1.3. Epidemiology

Six patients assured of a history of contact to live poultry, by another 5 patients denied a history of contact to live poultry. The epidemiologic data of the other 8 patients was not available.

1.4. Laboratory tests

WBC count was detected to have a decrease in 7 cases, being from 2.20 × 109/L to 7.11 × 109/L, with a mean of 4.69 × 109/L. Neutrophil percentage increased in 13 cases, but remained normal level in 6 cases, being from 63.0% to 92.9%, with a mean of 76.8%.

1.5. Diagnostic criteria of severe pneumonia

According to the diagnostic and treatment protocol for human infected avian influenza A (H7N9) established by National Council on Health and Family Planning Commission, P. R. China (edition, 2014), the cases with any one of the following criteria can be diagnosed as severe.

(1) Chest X-ray demonstrates lesions with multiple lobes involved or lesions progress more than 50% within 48 h;
(2) Difficulty breathing, with more than 24 breaths per minute;
(3) Severe hypoxemia, with oxygen flow at 3–5 L per minute and SpO2 $\leq$92%;
(4) Shock, ARDS or MODS (multiple organ dysfunction syndrome).

1.6. Pathological examination

Biopsy following percutaneous lung tissue puncture was performed in one case to observe the pathological changes. The pathogenic bacteria was observed after PAS and Masson staining. Acid-fast bacteria staining was performed to detect possible infection of *Mycobacterium tuberculosis*.

1.7. Radiological modality

Conventional chest X-ray was performed using Philips DiDi TH/VR, with the tube voltage 102 kV and automatic tube current. Bedside chest X-ray was performed using Hitachi Sirisu130HP mobile DR, with a tube voltage 100 kV and automatic tube current. CT scanning was performed using Toshiba TSX-101A 64-slice spiral CT, with a tube voltage 135 kV, automatic tube current, a pitch of 0.9, a matrix of 512 × 512, an FOV of 320 mm × 320 mm, a thickness of 5.0–6.0 mm, and an interval of 1 mm. CT scanning was from the apex to the bottom of lungs continuously. Lung window was reconstructed using conventional 1 mm and high resolution of 5 mm after the scanning.

1.8. Image analysis

All the images were independent analyzed by two radiologists with a title above associate chief-physician, and consensus was reached after consultation and discussion. The images were analyzed in terms of distribution and range of lesions, morphology of the lesions as well as changes of mediastinum and pleura.

2. Results

2.1. CT scans

(1) CT manifestations at the early phase (d 1–4 after onset)

The lesions more often onset from a lower lung lobe (17/19), only 2 cases had their lesions onset from an upper lung lobe. Poorly-defined patches of shadows and fragmental ground-glass opacities were demonstrated by CT scanning. Changes of pulmonary interstitium were observed, including interlobular septal thickening, acinar nodules, and other changes. Chest CT scanning demonstrated rapid progress of the lesions within a short period of 1–2 days, with rapid expansion, fusion, formation of large patchy opacities, and the lesions were demonstrated to involve multiple lobes (Fig. 1).

(2) CT manifestations at the evolving phase (d 5–10 after onset)

The lesions of 18 cases involved both lungs (18/19, 94.7%), and only 1 case showed lesions with unilateral lung involved (1/19, 5.3%). The lesions of 19 cases involved median lobe (lingual lobe) or lower lobe (19/19, 100%). The lesions of 18 cases involved 4 to 6 lung segments (18/19, 94.7%).

Ground-glass opacity was demonstrated by CT scanning in all 19 cases (100%), which were poorly defined in fragments and large patches. Pulmonary consolidation was also demonstrated in all 19 cases (19/19, 100%), which was more commonly found at the lower lung lobes to cross segments or

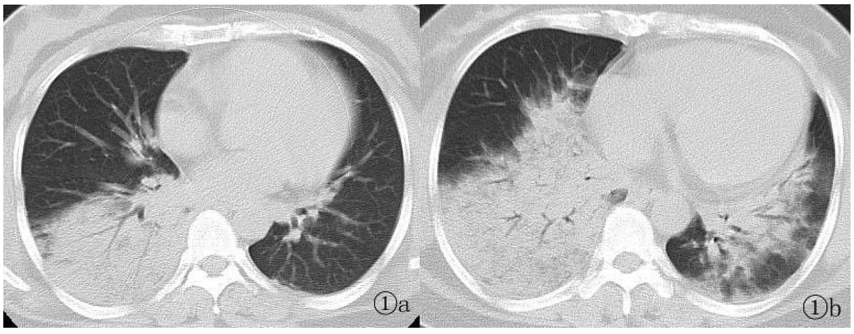

Fig. 1. A female patient aged 39 years was definitively diagnosed with severe pneumonia caused by human infected avian influenza A (H7N9). 1a) Chest CT scanning at d 4 after onset demonstrates large patchy consolidation at the right lower lung lobe, with observable air bronchogram; 1b) Chest CT scanning at d 6 after onset demonstrates substantial progress of the lesions, with large patchy consolidation and poorly defined patchy ground-glass opacities at lower lobes of both lungs and the right middle lung lobe.

lobes with higher density. Air bronchogram was observed in the area of consolidation. Air sacs in lungs were demonstrated in 3 cases (3/19, 15.8%), which were round with smooth lining, different sizes, various shapes and could be absorbed. Lymphadenectasis was demonstrated in 1 case (1/19, 5.3%), with several enlarged lymph nodes in the mediastinum, the larger one in front of the tracheal eminence, and the smaller one having a diameter of about 15 mm.Pleural effusion was demonstrated in 13 cases (13/19, 68.4%), mostly in a small quantity, 2 cases of unilateral and 11 cases of bilateral (Fig. 2).

(3) CT manifestations at the absorbing phase (d 11- after onset)

All the patients were admitted to our hospital at d 4–14 after onset (mean, 8.4 days), and by chest CT scanning, the lesions began to be absorbed at d 7–19 after onset, averagely at d 12.0 after onset. Interval between onset and beginning of absorption ranged from 1 day to 12 days, with an average of 3.7 days.

2.1.1. Absorption and prognosis

The group of 19 patients received antiretroviral and symptomatic therapies. In 1 patient, the lesions began to be absorbed at d 12 after admission to hospital, and in the remaining 18 patients, the lung lesions began to be absorbed at d 3 after hospitalization. During absorption, the range of

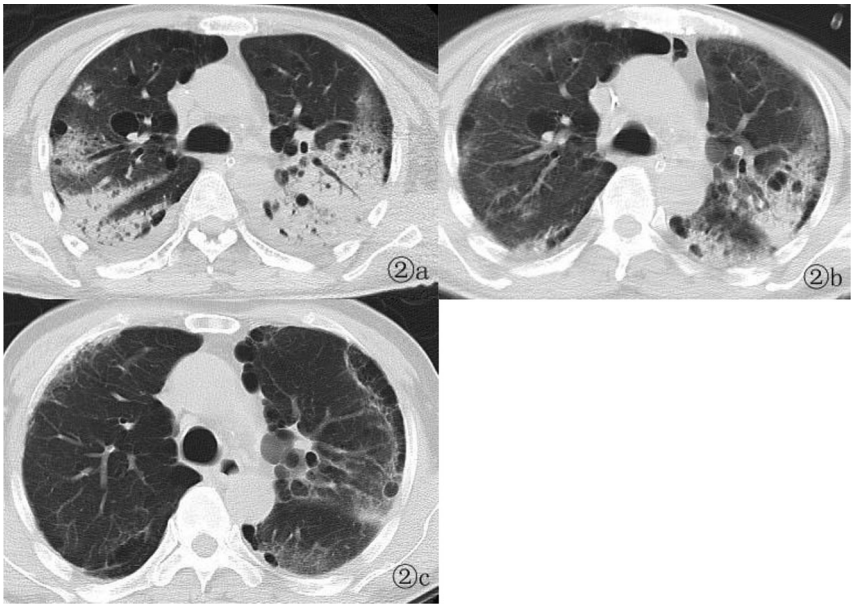

Fig. 2. A male patient aged 55 years was definitively diagnosed with severe pneumonia caused by human infected avian influenza A (H7N9). 2a) Chest CT scanning at d 9 after onset demonstrates multiples large patches of consolidation and ground-glass opacities in all the lobes of both lungs. Consolidations mainly distribute at the lower lobes and dorsal parts of both lungs. Air bronchogram and multiples air sacs are observable in the lesions. The left pleural cavity is demonstrated with a small quantity of effusion; 2b) Chest CT scanning at d 20 after onset demonstrates decreased range with consolidation at all lobes of both lungs with decreased density, multiple spatches of high-density shadows and ground-glass opacities. The lesions are demonstrated to have uneven density, mainly distributing at the lower lobes and the dorsal parts of both lungs. The air sacs show almost no changes, while effusion in the left pleural cavity is absorbed; 2c) Chest CT scanning at d 37 after onset demonstrates almost completely absorbed pulmonary consolidations, but patches of high-density shadows and ground-glass opacities. The remaining lesions mainly distribute under the pleura. The lungs are demonstrated with interstitial changes, pleura linear shadow, paraseptal emphysema and pleura bullas. The air sacs are shown to be decreased and effusion in the left pleural cavity is almost completely absorbed.

consolidation gradually reduced with decreased density, consolidation and recruitment of lung. The lesions at the upper and median lung lobes were absorbed earlier than those at the dorsal part of lower lung lobe and the subpleural lesions. The earlier emerging lesions were absorbed later, and vise versa. Finally, the residual lesions were more often located at dorsal part of the lower lung lobe and under the pleura.

In this group of patients, 18 were cured after hospitalization for 9–50 days (averagely 20.5 days). By CT scanning, consolidation disappeared in 14 cases (14/19, 73.7%); multiple patches of shadows were shown in 16 cases (16/19, 84.2%); lamellar ground-glass opacities were shown in 9 cases (10/19, 52.6%); linear shadows in 17 cases (17/19, 89.5%); latticed shadows and subpleural line in 7 cases (7/19, 36.8%); air sacs or pseudocavity, paraseptal emphysema, scar emphysema, subpleural bulla in 5 cases (5/19, 26.3%) (Fig. 2). Death occurred in 1 case due to respiratory and renal failure (Fig. 3).

2.2. Pathological findings

One case of this group received biopsy following percutaneous lung tissue puncture at the advanced period of the condition. Histopathology mainly showed fibrotic changes. Necrosis and abscission of some alveolar epithelia as well as reactive hyperplasia of alveolar epithelium were observed (Fig. 3c–d), but with no viral inclusions within epithelial cells. Slurry, cellulose, RBC, effused neutrophils, formation of hyaline membranes, squamous metaplasia and organizing exudates were observed in alveolar space (Fig. 3e). Some pulmonary alveoli were shown with atrophy or compensating emphysema. Pulmonary interstitial fibrosis, sometimes leukomonocyte, phlogocyte and reactive hematophagocyte were observable. Formation of hyaline thrombus and DIC were shown in capillary of pulmonary interstitium, sometimes with vascular occlusion (Fig. 3f). Empsyxis and secondary infection was sometimes found (Fig. 3).

3. Discussion

1. The CT manifestations characteristic of severe cases with pneumonia caused by human infected avian influenza A (H7N9).

Human infected avian influenza A (H7N9) is a newly emerging infectious disease caused by H7N9 subtype of avian influenza A virus. The disease was firstly reported in China in 2013, with main manifestations of flu-like symptoms such as fever, cough, and so on [3]. Severe pneumonia prompts critical condition, often in combination with ARDS, infectious shock, and so on. Chest CT scanning and diagnostic imaging are the important means for its clinical diagnosis and therapeutic evaluation [4]. This group of 19 cases with severe pneumonia caused by human infected avian influenza A (H7N9) had received more than three times of chest CT scanning. After comprehensive analysis, the CT manifestations of these patients include: (1) The lesions are more often found at the lower lung lobes, with 17 cases of this group showing lesions at 1 or 2 lower lung lobes. With progress of the disease, the lesions rapidly progress to involve multiple segments and lobes of both lungs, often 3 or more lung lobes up to all segments and lobes of both lungs. Pulmonary opacities are mainly located at the dorsal part of lungs. (2) Ground-glass opacities and pulmonary opacities are the cardinal imaging infestations to severe pneumonia caused by human infected avian influenza A (H7N9). When the condition is mild or at its early stage, the lesions are mainly ground-glass opacities. At the evolving phase, the percentage of pulmonary opacities increases, with air bronchogram in the pulmonary opacities. Ground-glass opacities mainly distribute at the anterior border of pulmonary opacities, showing as sporadic patchy opacities, even as “white lung” when in severe condition. The patient may develop significant hypoxemia, respiratory distress syndrome and respiratory failure. (3) Pleural effusion is also one of the imaging features of human infected avian influenza A (H7N9), with 13 cases of this group showing pleural effusion, and its incidence rate is higher than the previous report [5]. It may be related to the fact that all patients of this group suffered from severe pneumonia. The pleural effusion may be caused by systemic inflammatory response triggered by direct involvement of pleura by virus and/or virus evoked cytokine storm. (4) Pulmonary interstitial fibrosis is the main findings at the recovery phase, with all cases of this group showing as small patchy shadow under the pleura and/or at dorsal part of lower lobes. Fibriform cords, latticed shadows, fragmented ground-glass opacities and other pulmonary fibrosis are also CT changes. At the same time, in this group, subpleural paraseptal emphysema and ulotic emphysema, subpleural bullas and localized bronchiectasis are observable.

2. The relationship between CT manifestations and histopathological findings in the cases of severe pneumonia caused by human infected avian influenza A (H7N9).

Influenza virus is categorized into orthomyxovirus, and it is a single minus strand, segmental RNA virus that is enveloped [4]. The hemagglutinin in the tunica external of influenza virus A plays a key role in the pathomechanism of human infected avian influenza A (H7N9). Inflammatory factors may be mediate systemic inflammatory response syndrome and ARDS. Therefore, severe pneumonia is demonstrated as extensive ground-glass opacities and obvious consolidation by CT scan whose underlying mechanism is damaged pulmonary alveoli and pulmonary capillaries caused by virus, extensive effusion of pulmonary interstitium and pulmonary parenchyma [6]. Diffuse alveolar damage, interstitial fibrosis and air cavity extension, infiltration of leukomonocyte and plasma cells were demonstrated by histopathology. Therefore, the CT manifestations of severe pneumonia caused by human infected avian influenza A (H7N9) can be explained by the histopathologic findings as its pathomechanism. And, the main pathological changes of body organs are the result of phagocytosis of red blood cells, white blood cells and platelets by macrophages, known as reactive hemophagocytic syndrome. It can also explain different degrees of reduction of peripheral blood

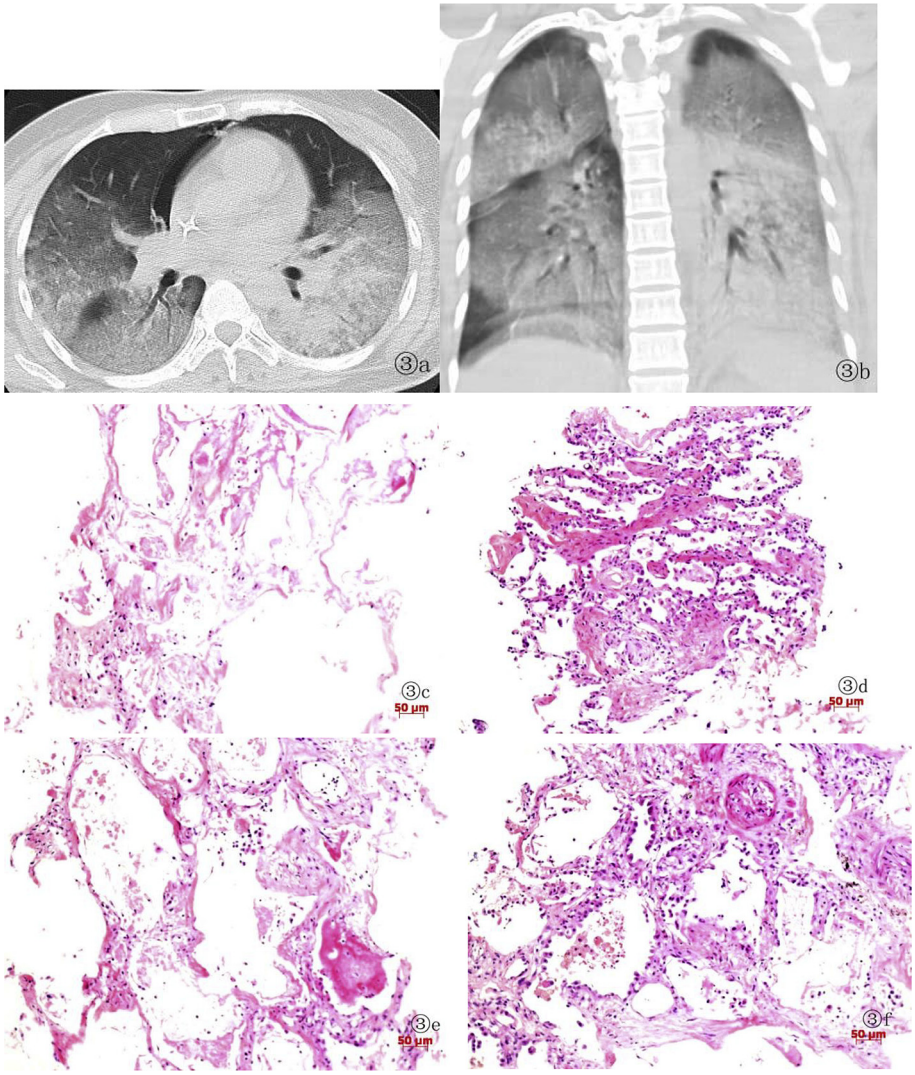

Fig. 3. A male patient aged 34 years was definitively diagnosed with severe pneumonia caused by human infected avian influenza A (H7N9), and this is the case that received biopsy following percutaneous lung tissue puncture. 3a–b) Chest CT scanning at d 12 after onset shows large patchy consolidation and ground-glass opacities in all lobes of both lungs, with poorly defined boundary. Air bronchogram is observable in the lesions, and mediastinal emphysema is demonstrated; 3c) The lung tissue is demonstrated to be degenerated and necrotic, with a few lymphocytes infiltrated; 3d)Reactive hyperplasia of the alveolar epithelium and pulmonary interstitial fibrosis are demonstrated; 3e)The alveolar epithelium is demonstrated to be dropped, with light red liquid, cellulose and a few lymphocytes in alveolar space; 3f) Alveolar epithelial cellsare demonstrated with hyperplasia, with some alveolar epithelium dropped and vascular occlusion observable.

counts by clinical laboratory tests at the early and evolving phases of severe pneumonia cause by human infected avian influenza A (H7N9). And the varying degrees damage of CD4T lymphocytes indicates immune responses.

3. The differential diagnosis of severe pneumonia caused by human infected avian influenza A (H7N9)

Severe pneumonia caused by human infected avian influenza A (H7N9) should be distinguished from influenza A (H1N1 or H5N1) and severe acute respiratory syndromes, and other conditions. Pneumonia caused by human infected avian influenza A (H1N1, H5N1 and H7N9) is all caused by influenza A virus, all with flu-like symptoms. The conditions are demonstrated as multiple ground-glass opacities in different sizes and consolidation by chest CT scan [7–10]. Compared to pneumonia caused by influenza A (H1N1), the lesions caused by H5N1 and H7N7 occupy a larger range and develop more rapidly, and air bronchogram is more common. The disease progressions of influenza H5N1 is rapid, following by H7N9 and H1N1. By CT scans, pneumonia caused by influenza A (H5N1) is mainly displayed as large patchy ground-glass opacities and consolidation at both lungs. The lesions distribute widely and progress rapidly [7,8]. In some cases, the lesions are erratic and absorbed slowly, with obvious pulmonary interstitial fibrosis and a mortality rate of about 59%. Onset from middle lobe and lower lobe of lungs, the lesions in the cases of human infected avian influenza A (H7N9) are mainly displayed as ground-glass opacities and lung consolidation, which change rapidly and are absorbed slowly, too [2,6,11], with a mortality rate of about 36%. The lesions are mainly displayed as multiple patchy ground-glass opacities

and patchy or large patchy high-density consolidation in the cases with influenza A (H1N1), with segmental atelectasis and pleural effusion [10,12] as well as a mortality rate of about 6%. Only based on radiological findings, the identification of infections by these different influenza viruses is challenging. And the differential diagnosis should be made in combination to epidemiological and etiological findings. Chest CT scans also display SARS as ground-glass opacities and lung consolidation, which progress rapidly with involvement of both lungs in about 50% of the patients, more often at middle and lower lung lobes. The lesions mainly distribute in the peripheral pulmonary tissue, with detectable interlobular septal thickening by high-resolution CT as broken paving-stones. Accompanying bronchiolectasis and a small quantity pleural effusion are also detectable [13]. These findings resemble to those of human infected avian influenza A (H7N9), but the interstitial changes in the cases of human infected avian influenza A (H7N9) are not obvious. The lesions of human infected avian influenza A (H7N9) show up in a more extensive range, with no obvious coverage at the peripheral pulmonary tissue. Epidemiological history and laboratory tests for its pathogen are the key to identify the two conditions.

Generally, severe pneumonia caused by human infected avian influenza A (H7N9) is demonstrated with ground-glass opacities and lung consolidation by chest CT scan. These lesions onset from middle and lower lobes of both lungs, and the condition may develop into pulmonary cavity or aerothorax, hydropneumothorax. The differential diagnosis for identification of influenza A virus (including H7N9, H5N1 and H1N1) is challenging based only on radiological findings. And their identification should be made in combination to epidemiological and etiological findings. Cross analysis of radiology and pathology is a way to further understand severe pneumonia caused by human infected avian influenza A (H7N9). And such a study is beneficial to clinical observation and evaluation of the condition, and is of great significance for disease control and mortality reduction.

References

[1] National Health and Family Planning Commission. Diagnostic and treatment protocol for human infections with avian influenza A (H7N9). edition, 2014. Beijing: National Health and Family Planning Commission; 2014.

[2] Lu PX, Zeng Z, Zheng FQ, Zheng GP, Zang J, Wang MX, et al. Characteristics of the imaging manifestations and dynamic changes in patients with severe pneumonia caused by H7N9 avian influenza virus. Radiol Pract 2014;29(7):740–4.

[3] Lu PX, Deng YY. Epidemiology and imaging manifestations of avian influenza. Imaging Pulm Infect 2010;16(5):431–4.

[4] Lu PX, Zhou BP. Clinical and imaging diagnosis of emerging infectious disease. Beijing: People's Medical Publishing House; 2013.

[5] Wang QL, Shi YX, Zhang ZY, Lu SH, Feng F, Zhu Y, et al. Preliminary imaging findings of novel reassortant avian-origin influenza A (H7N9) pneumonia. Chin J Radiol 2013;47(6):505–8.

[6] Huang XR, Huang H, Lu PX, Zeng Z, Chen XF, Zhou BP, et al. The correlation of CT manifestation, viral load and CD4+T lymphocyts in patients with H7N9 avian influenza pneumonia. Radiol Pract 2014;29(7):751–5.

[7] Lu PX, Zhu WK, Ye RX, Gong XL, Zang J, Yang GD, et al. CT manifestation and dynamic changes of grave pneumonia in adults caused by H5N1 subtype of human avian influenza virus. Chin J CT MRI 2007;5(15):31–4.

[8] Lu PX, Zhou BP, Zhu WK, Chen XC, Ye RX, Zheng GP. Imaging features of pneumonia caused by highly pathogenic H5N1 subtype human avian influenza virus. Chin J Med Imaging Technol 2007;23(4):532–5.

[9] Zhou BP, Li YM, Lu PX. Human avian influenza. Beijing: Science Press; 2007.

[10] Yang GD, Lu PX, Cao Y, Zhang LP, Li Y, Li SZ, et al. Types and manifestations in CT images of pneumonia caused by influenza A (H1N1). Guangdong Med J 2010;31(21):2822–3.

[11] Zeng Z, Lu PX, Zhou BP, Liu YX, Yuan J, Li GB, et al. Imaging manifestations of the severe cases of pneumonia caused by H7N9 subtype human avian influenza virus. J Tuberc Lung Health 2014;3(1):25–8.

[12] Deng YY, Lu PX, Yang GL, Liu WL, Liu YX, Ye RX, et al. Correlative study of semi-quantitative score of chest CT findings and viral load in novel influenza A (H1N1) virus infection. Radiol Pract 2010;25(9):965–8.

[13] Lu PX, Yang GD, Yu WY, Yuan MY, Gong XL, Liu JQ, et al. Imaging diagnosis of SARS. J Clin Pulm Med 2003;8(4):295–8.